affords excellent dispersion and control, wide particle size latitude, and smooth, uniform spheres without the need for surfactants. More importantly, because glutaraldehyde is presented to the aqueous albumin microsphere dispersion from the organic phase, there must be a strong preference for aldehyde-amino group reactions and cross-linking at or near the albumin surface. This probably produces a case-hardening effect with a higher cross-link density near the surface of the microspheres accompanied also by a much higher concentration of mono-reacted dialdehyde at the surface (Scheme III). The result of monofunctional glutaraldehyde capping of lysine amino groups at the albumin microsphere surface would be to increase surface anionicity and hydrophilicity, especially if a portion of the free aldehyde functions oxidize to carboxyl groups.

The availability of a relatively high surface concentration of aldehyde functionality also facilitates a variety of chemical modifications including: aminoalcohol capping to enhance hydrophilicity; enzyme, antibody, or other protein ligand binding; covalent attachment of amino-functional drugs. As suggested in Scheme III, such changes in surface functionality may be used to enhance tissue immobilization by covalent or physical binding, for specific tissue targeting using biospecific affinity ligands (*e.g.*, tumor-specific antibodies), or for improved diagnostic or immune assay reagents and procedures.

REFERENCES

(1) J. Heller and R. W. Baker, "Controlled Release of Bioactive Materials," Academic, New York, N.Y., 1980, pp. 1, 17.

(2) E. P. Goldberg, Ed., in "Targeted Drugs," Wiley, New York, N.Y., 1982.

(3) D. S. T. Hsieh, R. Langer, and J. Folkman, *Proc. Natl. Acad. Sci. USA*, **78**, 1863 (1981).

(4) G. Gregoriadis, *Pharmacol. Ther.*, **10**, 103 (1980).

(5) U. Zimmerman, in "Targeted Drugs," E. P. Goldberg, Ed., Wiley, New York, N.Y., 1982.

(6) T. M. S. Chang, in "Polymer Grafts in Biochemistry," H. F. Hixson and E. P. Goldberg, Eds., Marcel Dekker, New York, N.Y., 1976, pp. 245, 258.

(7) I. S. Joholm and P. Edman, *J. Pharmacol. Exp. Ther.*, **211**, 656 (1979).

(8) K. J. Widder, A. E. Senyei, and D. F. Ranny, "Advances in Pharmacology and Chemotherapy," Academic, New York, N.Y., 1979, pp. 213, 271.

(9) A. F. Yapel, U.S. Patent 4,147,767, (1979).

(10) P. A. Kramer, *J. Pharm. Sci.*, **63**, 1646 (1974).

(11) J. Koch-Weser and E. M. Sellers, *N. Engl. J. Med.*, **294**, 311 (1976).

(12) *Ibid.*, **294**, 526 (1976).

(13) K. J. Widder, A. E. Senyei, and D. F. Ranney, *Cancer Res.*, **40**, 3512 (1980).

(14) T. Ishizaka, K. Endo, and M. Koishi, *J. Pharm. Sci.*, **70**, 358 (1981).

(15) A. E. Senyei, S. D. Reich, C. Gonczy, and K. J. Widder, *ibid.*, **70**, 328 (1981).

(16) K. Widder, G. Flouret, and A. Senyei, *ibid.*, **68**, 79 (1979).

(17) E. P. Goldberg, R. N. Terry, and M. Levy, *Am. Chem. Soc. Preprints*, Div. Org. Coatings Plastics Chem., **44**, 132 (1981).

(18) R. N. Terry, M. S. Thesis, University of Florida (1980).

(19) E. P. Goldberg, H. Iwata, R. N. Terry, W. E. Longo, M. Levy, and J. L. Cantrell, in Affinity Chromatography and Related Techniques," Gribnau, Visser, and Nivard, Eds., Elsevier, Amsterdam, 1982, p. 375.

(20) E. Rswicki, T. R. Hauser, T. W. Stanley, and W. Elbert, *Anal. Chem.*, **33**, 93 (1961).

(21) Y. Ikada, H. Iwata, T. Mita, and S. Nagaoka, *J. Biomed. Mater. Res.*, **13**, 607 (1979).

(22) T. K. Lee, T. D. Sokoloski, and G. P. Royer, *Science*, **213**, 233 (1981).

ACKNOWLEDGMENTS

This work was supported in part by the State of Florida Biomedical Engineering Center.

The authors thank Dr. B. Dunn for use of his scintillation counter, Dr. G. Onoda for use of the Coulter counter, and M. Smith for the preparation of this manuscript.

Kinetics and Mechanism of the Equilibrium Reaction of Triazolam in Aqueous Solution

MASAHARU KONISHI ˣ, KENTARO HIRAI ‡, and YOSHIO MORI *

Received October 6, 1981, from the **Division of Analytical Chemistry* and the ‡*Division of Organic Chemistry, Shionogi Research Laboratories, Shionogi & Co., Ltd., Fukushima-ku, Osaka 553, Japan.* Accepted for publication January 11, 1982.

Abstract □ The equilibrium kinetics of triazolam in aqueous solution was investigated in the pH range of 1–11 at body temperature. The quantitative study indicated that it forms equilibrium mixtures consisting of ring-opened and closed forms with the composition being dependent on pH. The equilibrium constants of the two species in the pH range studied were determined by GLC method. The apparent first-order rate constants were estimated from the decreasing or increasing absorbance of the mixture in solutions. The forward-reaction rate constant (k_f) showed a bell-shaped k_f–pH profile with a rate maximum at pH 4.59, which indicates not only that the carbinolamine intermediate forms during the equilibrium reaction, but that the rate-determining step of the reaction differs for the acidic and basic sides of the rate maximum. The reverse-reaction rate constant decreased with increasing pH and could not be estimated in the pH region >5.65. Theoretical curves for both forward and reverse reactions satisfactorily fit the observed data. The pKa values of triazolam and its opened-form amine were estimated to be 1.52 and 6.50, respectively.

Keyphrases □ Triazolam—kinetics, mechanism of equilibrium in aqueous solution □ Kinetics—triazolam, mechanism of equilibrium in aqueous solutions □ Equilibrium reaction—triazolam, kinetics, mechanism in aqueous solutions

1,4-Benzodiazepines, first synthesized in the early 1960s, are important minor tranquilizers. These tranquilizers are being extensively used as sedative, hypnotic, muscle relaxant, and anticonvulsant drugs. Their stability and reactivity in aqueous solutions have been under study extensively in the last 5 years. Reaction mechanisms for the hydrolysis of 1,4-benzodiazepines have been reported for chlordiazepoxide (1, 2), oxazepam (3), diazepam (4), nitrazepam (4, 5), desmethyldiazepam (6), and clonazepam (6). Furthermore, equilibrium reactions of these compounds have been reported for pyrazolodiazepinone (7), diazepam (8), nitrazepam (9), triazolobenzodiazepines (10), flunitrazepam (11), and desmethyldiazepam (12). It is now well known that hydrolysis of an azomethine bond

0022-3549/82/1200-1328$01.00/0

in acidic solution gives the corresponding aminobenzophenone, which reversibly cyclizes into the original form in alkaline medium. Namely, 1,4-benzodiazepines exist as pH-dependent equilibrium mixtures of ring-opened and closed forms. However, no extensive, detailed study on the mechanism of the equilibrium reaction has been reported.

This study describes the mechanism of the equilibrium reaction between triazolam and its opened form in an aqueous solution.

EXPERIMENTAL

Materials—2′,5-Dichloro-2-(3-aminomethyl-5-methyl-4H-*s*-triazol-4-yl) benzophenone (I), 8-chloro-1-methyl-6-(*o*-chlorophenyl)-4H-*s*-triazolo[4,3-*a*] 1,4-benzodiazepine (triazolam, II), 4-amino-7-chloro-5-(2-chlorophenyl)-1-methyl-4H-*s*-triazolo[4,3-*a*] quinoline (III), and 3-amino-6-chloro-4-(2-chlorophenyl)-1-*n*-propylquinolin-2-one (IV) were synthesized. Dotetracontane was purchased from a commercial source[1]. All other reagents and solvents were of reagent grade and were used without further purification. Deionized water was further distilled before use in the aqueous solutions.

Equipment—UV spectra were recorded using a spectrophotometer[2] equipped with a thermostatically controlled cell holder. The pH was measured with a pH meter[3] at the temperature of the study.

TLC was done with a precoated 0.25-mm silica gel TLC plate[4] using a developing solvent system of chloroform–acetone–ethanol (3:1:1).

The gas chromatograph[5] was equipped with a 10-mCi ^{63}Ni-electron-capture detector (ECD) or a flame ionization detector (FID). The column was coiled glass (0.5 m × 3-mm i.d.), packed with 3% OV-17 on 100–120 mesh Gas Chrom Q[6]. The carrier gas was ultrapure nitrogen flowing at a rate of 60 ml/min. Temperature settings during operation were 320° for the injection port and detector and 290° for the column. Peak heights of the compounds were determined using an integrator[7]. Under these GC conditions, the retention times for the compounds under study were 2.25 min for II, 3.35 min for III, 0.9 min for IV, and 6.15 min for dotetracontane.

Kinetic Studies—All rate studies were performed in aqueous buffer solutions at 37.0 ± 0.1°. The buffer systems used were: pH 1.1–5.6, acetate; pH 6–8, phosphate; pH 9–10, borate; and pH 11–12, phosphate. The ionic strength of each was adjusted to 0.5 with potassium chloride.

The compound to be studied was dissolved in ethanol and diluted (1:20) with preincubated buffer solution kept at 37° to make a 10^{-4} *M* solution. Next, an appropriate volume of the solution was pipeted into the UV cell, and the reaction was followed spectrophotometrically by reading the decrease or increase in absorbance at 264 nm.

Reactions starting from I were studied in the pH range of 1.92–11.44. The sum of the first-order rate constants for the forward and reverse reactions (k_f and k_r) was determined from linear plots of ln $(A_t - A_\infty)$ *versus* time by the least-squares method (Eq. 1), where A_t, A_∞, and A_0 are the absorbance at time t, infinity, and time 0, respectively:

$$\ln(A_t - A_\infty) = \ln(A_0 - A_\infty) - (k_f + k_r)t \qquad \text{(Eq. 1)}$$

Reactions initiating from II were studied in the pH region of 1.13–1.40. The sum of the first-order rate constants for the forward and reverse reactions was obtained from the linear plots of ln $(A_\infty - A_t)$ against time by the least-squares method (Eq. 2), where A_∞, A_t, and A_0 are the absorbance at infinity, time t, and time 0, respectively:

$$\ln(A_\infty - A_t) = \ln(A_\infty - A_0) - (k_f + k_r)t \qquad \text{(Eq. 2)}$$

Product Identification—For the identification studies, 2×10^{-3} *M* solutions of I were prepared using 0.5 *N* NaOH solution, the pH 6.5 buffer solution, and a 0.01 *N* HCl solution. These solutions were left standing at room temperature for 15 hr, then a 5-ml sample was taken from each solution and was subjected to extraction with dichloroethane for TLC analysis. The chromatograms were visualized under UV light and iodine vapour to identify the products. Dichloroethane solutions of reference standards were spotted directly on the TLC plates.

Determination of I and II in Aqueous Solutions—*ECD-GC Method*—In this method, caution was paid to determine the compounds without disturbing the equilibrium. The triazoloaminoquinoline derivative (III) was derived by acetylation followed by cyclization to obtain a suitable compound for GC as shown in Scheme I.

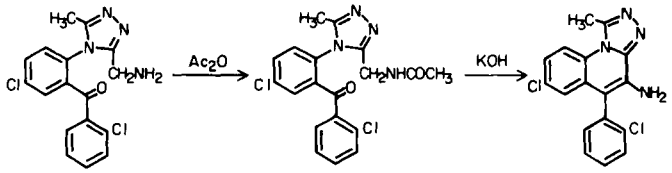

I III

Scheme I

The pH 11 phosphate buffer (containing 0.2 *M* Na_2HPO_4) was added to 1 ml of reaction solution (initially containing 2×10^{-4} *M* of I) to make a 10-ml solution at pH 10, with the temperature kept at 0° with ice (quenched solution). This quenching procedure was necessary to prevent disturbance of the equilibrium mixture during assay. Triethylamine (0.2 ml), 2 *N* KOH (1 ml) quenched reaction solution (1 ml), and acetic anhydride (0.1) were added with ice cooling to a 12-ml centrifuge tube containing 3 ml of dichloroethane. After this mixture was shaken for 15 min on a mechanical shaker (for acetylation of I), 1 ml of the dichloroethane solution was transferred to another 12-ml centrifuge tube by Eppendorf pipet and evaporated to dryness. To dissolve the residue, 0.2 ml of ethanol was added followed by 2 ml of 2 *N* KOH and the solution was heated for 3 hr at 91 ± 1° (cyclization to III). After it had cooled, the reaction solution was extracted with 5 ml of benzene containing 1 μg of IV as an internal standard for 5 min, then 2 μl of the benzene layer was subjected to ECD-GC. Calculation was done by the internal standard method using the peak height ratios. Recoveries of I for the acetylation and the cyclization were 80 and 83.9%, respectively, and the overall recovery was 60.0% (n = 36, CV = 3.30%). Recovery of II was 86.7% (n = 27, CV = 4.64%) in this procedure.

FID-GC Method—In the equilibrium solutions, if the weight ratios of II to I were >5, separation of the peaks of Compounds II and III on ECD-GC was difficult because of low resolution. This problem was overcome by using the FID-GC, in which no peak broadening of Compound II was observed. The quantities of I and II were determined by separate procedures.

For Compound I, 5.7 ml of the pH 11 phosphate buffer and 0.3 ml of 1 *N* KOH were added to 4 ml of reaction solution (initial concentration of I: 4×10^{-4} *M*) to make a 10-ml solution of pH 10, keeping the temperature at 0° with ice (quenched Solution I). Quenched Solution I (2.5 ml) and acetic anhydride (0.1 ml) were added with ice cooling to a 12-ml centrifuge tube containing 3 ml of dichloroethane, 0.2 ml of triethylamine, and 1 ml of 2 *N* KOH. The mixture was shaken for 15 min, then the dichloroethane layer was transferred to another 12-ml centrifuge tube and evaporated to dryness. Next, 0.2 ml of ethanol was added to dissolve the residue and 2 ml of 2 *N* KOH was added to this solution, which was then heated for 3 hr at 91 ± 1°. After cooling, the reaction solution was subjected to extraction for 5 min with a mixture of 4 ml of benzene and 1 ml of *n*-hexane containing 3.5 μg of dotetracontane as an internal standard, then the resulting organic layer was transferred to a 30-ml round-bottom flask and evaporated to dryness. The residue was dissolved in 0.1 ml of solvent (acetone–*n*-hexane, 1:2) and 4 μl of the solution was subjected to FID-GC. Recovery of I was 64.3% (n = 18, CV = 2.94%).

For Compound II, the pH 11 phosphate buffer was added to 1 ml of reaction solution (the same solution as that for Compound I) to make a 10-ml solution of pH 10 with ice cooling (quenched Solution II). Quenched Solution II and acetic anhydride (1 ml) were added with ice cooling to a 12-ml centrifuge tube containing 3 ml of dichloroethane, 0.2 ml of triethylamine, and 1 ml of 2 *N* KOH. The mixture was shaken for 15 min, then the dichloroethane layer was removed by pipeting and evaporated to dryness. The residue was dissolved in 0.2 ml of ethanol and 2 ml of 2 *N* KOH, and the solution was subjected to extraction with a mixture of 4 ml of benzene and 1 ml of *n*-hexane containing 35 μg of dotetracontane for 5 min. The organic layer was transferred to a 30-ml round-bottom flask and evaporated to dryness. The residue was dissolved in 0.5 ml of solvent (acetone–*n*-hexane, 1:2) and 2 μl of this solution was subjected to FID-GC. Recovery of Compound II was 81.1% (n = 10, CV = 2.34%).

[1] Milton Roy, Fla.
[2] Model 323, Hitachi, Japan.
[3] Model $F7_{ss}$, Hitachi-Horiba, Japan.
[4] G60, F_{254}, E. Merck, G.F.R.
[5] Model GC-7A, Shimadzu, Japan.
[6] Milton Roy, Fla.
[7] Model C-R1A, Shimadzu, Japan.

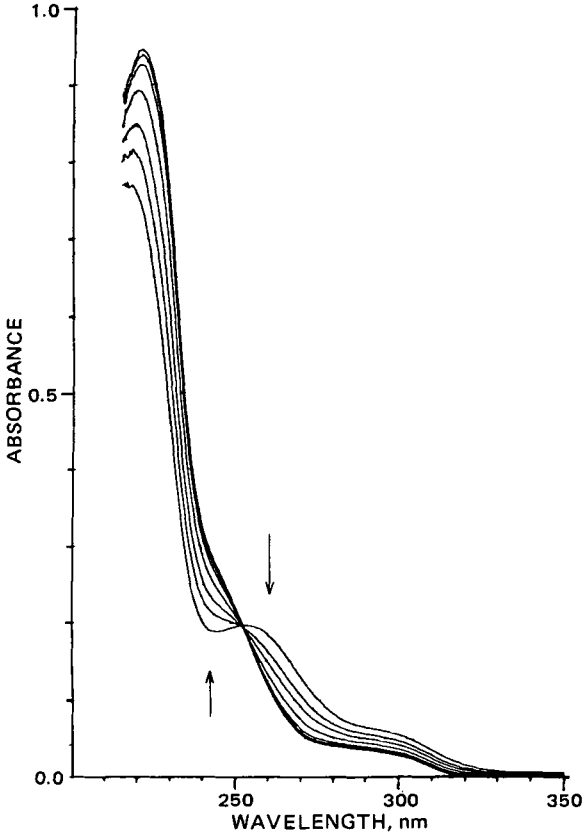

Figure 1—*Typical spectral changes due to the ring-closure reaction of Compound I (× 10^{-4} M) into triazolam in 0.1 M acetate buffer, pH 5.65 (μm = 0.5) at 37°. Spectra were measured at 5, 13, 20, 35, 60, 85, and 150 (∞) min after initiation of the reaction.*

RESULTS AND DISCUSSION

Spectral Change and the Nature of the Reaction—After the pH 6.5 buffer solution and the 0.5-*N* NaOH solution of I had been left standing for several hours, both showed only one spot with an R_f value (0.68) identical to that of II on TLC (R_f for I was 0.18 in this system). The chromatogram for the standing solution of I in 0.01 *N* HCl gave two spots, identical to I and II, of compounds present in approximately equivalent amounts.

The UV spectral change of I in the pH 5.65 buffer at 37° is shown in Fig. 1. Immediately after I had dissolved, the absorption spectrum showed an absorption maximum (λ_{max}) at 257 nm, which decreased concurrently with time. At infinity, the shape of the redundant spectrum was identical to that of II in the same medium. An isosbestic point at 253 nm was observed during the reaction. On the other hand, the spectral change of II in 0.1 *N* HCl showed a reverse change in which the absorption at λ_{max} increased with time when the isosbestic point was kept at 253 nm; the final spectrum could be superimposed on that of I in the same solution. Furthermore, the spectrum of II obtained by mixing the equilibrium pH 5.65 solution of II and 1 *N* HCl rapidly changed into a spectrum similar to that of II in 0.1 *N* HCl solution.

These observations indicate that I and II in these aqueous solutions undergo reversible reactions involving cyclization and hydrolytic azomethine bond cleavage, respectively, to produce equilibrium mixtures of Compounds I and II (Scheme II), as in the case of estazolam (10).

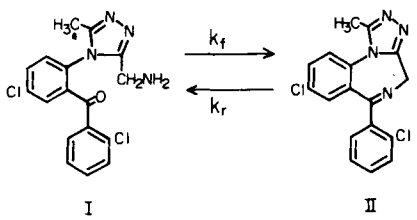

I II

Scheme II

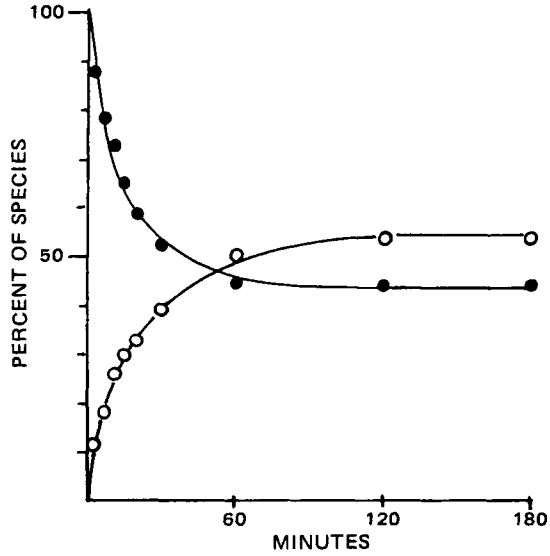

Figure 2—*Time courses for Compound I (●) and triazolam (○) in a 0.2 M acetate buffer, pH 2.30 (μm = 0.5) at 37° initially containing 2 × 10^{-4} M of Compound I.*

Cyclization of I to II and Quantitative Aspects—The equilibrium mixture of I and II was analyzed quantitatively by GC procedure. The result obtained for the 0.2 *M* acetate buffer solution of pH 2.3 (initial concentration of I: 2 × 10^{-4} *M*) is shown in Fig. 2. The data plotted as the percent of I and of II with time showed a continuous decrease and increase, respectively. During the time course of the equilibrium reaction, the total recoveries of I plus II were >98% based on the initial concentration of I. Moreover, the rate of decrease for I was equivalent to the rate of increase for II. These results also support the fact that both I and II exist as equilibrium mixtures in solution.

Effect of pH on the Equilibrium Constant—The apparent equilibrium constant, *K*, is defined by Eq. 3, where $[I]_\infty$ and $[II]_\infty$ are the molar concentrations of I and II at equilibrium, and k_f and k_r are first-order rate constants of the forward and reverse reaction, respectively:

$$K = \frac{[II]_\infty}{[I]_\infty} = \frac{k_f}{k_r} \qquad \text{(Eq. 3)}$$

The value for *K* was determined at various pH values over the range of pH 1.13–11.44 at 37° by determining the components of the reaction solutions after they had attained equilibrium state. The results are shown in Table I. The *K* values increased with increasing pH and became >400 at pH >5.02.

When equilibrium is attained at any pH, the fractions of I (F_I) and II (F_{II}) in the reaction solutions are defined by Eqs. 4 and 5. The plots of the fractions of the individual species against pH are shown in Fig. 3. F_I

Table I—Equilibrium and Rate Constants of Ring-Closing and Ring-Opening Reactions in Aqueous Buffer Solutions [a]

pH	a_{H^+}	*K*	$k_{obs} \times 10^{-2}$/min		
			k_{app}	k_f	k_r
1.13	7.41 × 10^{-2}	0.18	14.8	2.30	12.5
1.40	3.98 × 10^{-2}	0.26	11.2	2.31	8.89
1.92	1.20 × 10^{-2}	0.61	6.81	2.58	4.23
2.30	5.01 × 10^{-3}	1.2	4.99	2.72	2.27
2.68	2.09 × 10^{-3}	2.4	4.20	2.96	1.24
3.13	7.41 × 10^{-4}	5.4	3.99	3.37	0.623
3.39	4.07 × 10^{-4}	15	3.91	3.67	0.244
3.90	1.26 × 10^{-4}	48	4.04	3.96	0.082
4.59	2.57 × 10^{-5}	230	4.37	4.35	0.019
5.02	9.55 × 10^{-6}	400	4.24	4.23	0.011
5.65	2.24 × 10^{-6}	>400	3.65	3.65	—
6.25	5.62 × 10^{-7}	>400	2.79	2.79	—
7.12	7.59 × 10^{-8}	>400	1.11	1.11	—
7.74	1.82 × 10^{-8}	>400	0.682	0.682	—
8.75	1.78 × 10^{-9}	>400	0.461	0.461	—
9.76	1.74 × 10^{-10}	>400	0.412	0.412	—
10.47	3.39 × 10^{-11}	>400	0.401	0.401	—
11.44	3.63 × 10^{-12}	>400	0.473	0.473	—

[a] μ = 0.5, at 37°.

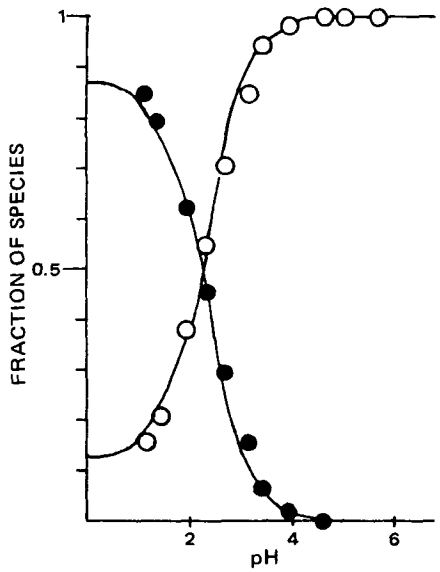

Figure 3—*Plot of the composition of the equilibrium mixture consisting of Compound I (●) and triazolam (○) versus pH at 37°. Solid lines are values calculated using Eqs. 4, 5, and 23.*

decreases with increasing pH from 0.85 at pH 1.13 to <0.002 at pH >5.02 at which the equilibrium mixture contains >99.8% of ring-closed Compound II.

$$F_I = \frac{[I]_\infty}{[I]_\infty + [II]_\infty} = \frac{1}{1+K} \quad \text{(Eq. 4)}$$

$$F_{II} = 1 - F_I = \frac{K}{1+K} \quad \text{(Eq. 5)}$$

Rate Constant Determination and Rate–pH Profiles—Semilogarithmic plots of $(A_t - A_\infty)$ against time for the equilibrium reaction in various pH solutions are shown in Fig. 4. In the pH region studied, all the plots displayed strict first-order kinetics for >5 half-lives. The apparent first-order rate constants (k_{app}) are expressed as Eq. 6. Each rate constant for the forward and reverse reactions can be derived from Eqs. 3 and 6.

$$k_{app} = k_f + k_r \quad \text{(Eq. 6)}$$

In Fig. 5, the first-order rate constants for the formation and the hydrolysis of II at 37°, which were extrapolated to zero buffer concentration, are plotted against pH.

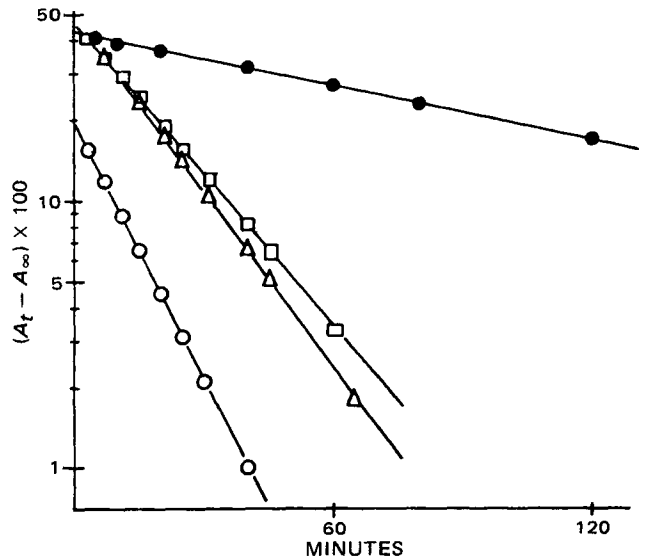

Figure 4—*Typical apparent first-order plots for the equilibrium reaction between Compound I and triazolam at 37°, μm = 0.5. Key: (○) pH 1.92; (△) pH 5.02; (□) pH 3.39; (●) pH 7.74.*

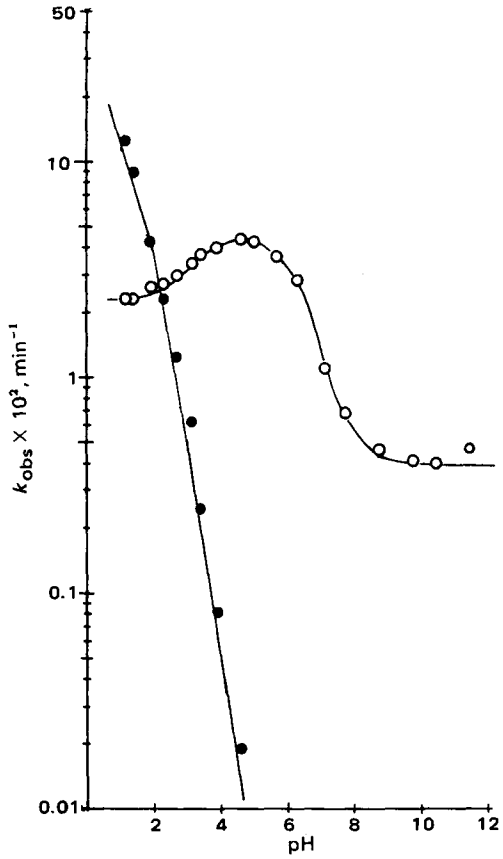

Figure 5—*Log k–pH profile for the equilibrium reaction consisting of forward (○) and reverse reactions (●) at 37°, μm = 0.5. Solid lines were based on calculations using Eq. 18 or Eq. 22. All rates are extrapolated to zero buffer concentration.*

For the formation rate, a maximum occurs near pH 4.5. On the alkaline side of the pH–rate maximum (pH 4.5–9), the rate increases with increasing acidity, suggesting that an acid-catalyzed reaction is predominant. In the solution at pH >9, the rate becomes constant. On the acidic side of the pH–rate maximum, the rate decreases with increasing acid concentration and becomes independent of pH at pH <1.40, indicating the existence of a specific acid-catalyzed reaction as well as an uncatalyzed one of the free form of I.

The hydrolysis of II shows an acid-catalyzed reaction over the pH range used in this study and its rate could not be determined ≥pH 5.65 because the equilibrium constants were too large to be determined.

General Reaction Mechanism—Reactions of carbonyl compounds with amines have been reviewed previously (13–15). Moreover, a noteworthy series of papers have reported on studies of the formation of semicarbazones (16, 17), Schiff base (18, 19), and oxime (16) in aqueous solutions. These studies have pointed out that the formation and hydrolysis of these compounds proceed by a two-step mechanism involving a tetrahedral carbinolamine intermediate. The evidence for the two-step mechanism is based on the results that the Schiff base formation undergoes a transition in the rate-determining step from the dehydration of the carbinolamine intermediate at neutral pH to the amine attack under acidic conditions. Formation of II exhibits a pH–rate maximum similar to that in the formation of oxime (16) and *N*-*p*-chlorobenzylideneaniline (18). Therefore, the formation and the hydrolysis of II are considered to proceed by the two-step reaction mechanism, as shown:

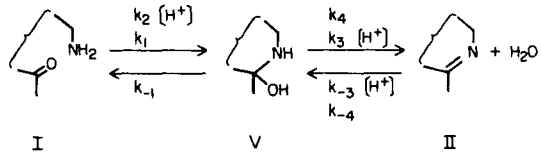

Scheme III

In the forward reaction, the acid-catalyzed dehydration of the carbinolamine intermediate (V) at nearly neutral pH determines the rate

which may account for a leveling off, but not a decrease in the rate with increasing pH. At low pH values, the rate of dehydration becomes very fast, and at the same time, the rate of the amine attack is retarded because of the conversion of the free amine form of I into its conjugate acid. Consequently, a change in the rate-determining step occurs and the attack of the amine becomes rate-determining, accounting for the observed decrease in the rate on the acid side of the pH–rate maximum.

In the reverse reaction, the hydrolysis rates are measurable only on the acidic side of the pH–k_f maximum. The rate-determining step of this reaction in this pH region is the cleavage of the C—N bond from V to I. Since the carbinolamine intermediate is formed by a water molecule attack at the conjugate acid of II, the hydrolysis rate is directly proportional to the concentration of the conjugate acid as an active acidic species of II.

In Scheme III, k_1 and k_{-1} represent uncatalyzed reaction rate constants; k_2, k_3, and k_{-3} represent acid-catalyzed rate constants; and k_4 and k_{-4} represent water-catalyzed rate constants. When a steady-state approximation is applied to the carbinolamine intermediate, the rate equations for the forward and the reverse reaction can be written as Eqs. 7 and 8, respectively; where a_{H^+} is hydrogen ion activity; K_I and K_{II} are dissociation constants for the conjugate acid of I and II:

$$k_{f(obs)} = \frac{K_I(k_1 + k_2a_{H^+})\,(k_3a_{H^+} + k_4)}{(K_I + a_{H^+})\,(k_{-1} + k_3a_{H^+} + k_4)} \qquad \text{(Eq. 7)}$$

$$k_{r(obs)} = \frac{k_{-1}a_{H^+}\,(k_{-3}a_{H^+} + k_{-4})}{(K_{II} + a_{H^+})\,(k_{-1} + k_3a_{H^+} + k_4)} \qquad \text{(Eq. 8)}$$

Formation Mechanism—On the alkaline side of the rate maximum (Fig. 5), the rate-determining step should be the dehydration from the carbinolamine intermediate. This implies $k_{-1} \gg (k_3a_{H^+} + k_4)$; therefore, Eq. 7 can be reduced to Eq. 9:

$$k_{f(obs)} = \frac{K_I(k_1 + k_2a_{H^+})\,(k_3a_{H^+} + k_4)}{k_{-1}(K_I + a_{H^+})} \qquad \text{(Eq. 9)}$$

If k_1 is assumed to be much larger than $k_2a_{H^+}$, Eq. 10 will be obtained:

$$k_{f(obs)} = \frac{k_1K_I(k_3a_{H^+} + k_4)}{k_{-1}(K_I + a_{H^+})} \qquad \text{(Eq. 10)}$$

In Eq. 10, two pH regions, $k_3a_{H^+} \gg k_4$ and $K_I \gg a_{H^+}$ are considered. In the former, Eq. 11 can be derived:

$$k_{f(obs)} = \frac{k_1k_3K_Ia_{H^+}}{k_{-1}(K_I + a_{H^+})} \qquad \text{(Eq. 11)}$$

When both sides of Eq. 11 are divided by a_{H^+} and the equation is converted into its reciprocal form, Eq. 12 is obtained:

$$a_{H^+}/k_{f(obs)} = \frac{k_{-1}}{k_1k_3K_I}a_{H^+} + \frac{k_{-1}}{k_1k_3} \qquad \text{(Eq. 12)}$$

Consequently, k_{-1}/k_1k_3 and K_I can be obtained from the plot of $a_{H^+}/k_{f(obs)}$ against a_{H^+}. The linear relationship between $a_{H^+}/k_{f(obs)}$ and a_{H^+} is shown in Fig. 6. From the extraordinate intercept and the slope of the linear plot, k_1k_3/k_{-1} and K_I were 1.39×10^5/min and 3.13×10^{-7} ($pK_I = 6.50$), respectively. Furthermore, since a_{H^+} was much larger than K_I at the pH which gave the rate maximum, Eq. 11 could be reduced to:

$$k_{f(max)} = \frac{k_1}{k_{-1}}k_3K_I \qquad \text{(Eq. 13)}$$

Putting the parameter obtained from Fig. 6 into Eq. 13, $k_{f(max)}$ was estimated to be 4.35×10^{-2}/min, which agreed with the observed data.

In the case of $K_I \gg a_{H^+}$, Eq. 10 can be reduced to Eq. 14.

$$k_{f(obs)} = \frac{k_1}{k_{-1}}k_3a_{H^+} + \frac{k_1}{k_{-1}}k_4 \qquad \text{(Eq. 14)}$$

Further, if k_4 is $>k_3a_{H^+}$, the following equation can be derived:

$$k_{f(obs)} = \frac{k_1}{k_{-1}}k_4 \qquad \text{(Eq. 15)}$$

Equation 15 indicates that the formation rate becomes constant in a high pH region when $K_I \gg a_{H^+}$ and $k_4 \gg k_3a_{H^+}$. From the observed data, k_1k_4/k_{-1} was calculated to be 0.4×10^{-2}/min. The value k_4/k_3 obtained by dividing k_1k_4/k_{-1} by k_1k_3/k_{-1} was 2.88×10^{-8}. This inductively proves that Eq. 15 can be used to explain the constant value of k_f at the pH region >9, because $k_4 \gg k_3a_{H^+}$ is valid in these pH solutions.

The assumption that the rate-determining step of the reaction of the acidic side of the rate maximum changes to attack of the free amine is equivalent to the statement: $(k_3a_{H^+} + k_4) \gg k_{-1}$. Therefore, Eq. 7 is reduced to:

$$k_{f(obs)} = \frac{K_I(k_1 + k_2a_{H^+})}{K_I + a_{H^+}} \qquad \text{(Eq. 16)}$$

In the pH region under discussion, $a_{H^+} \gg K_I$, and Eq. 17 is obtained:

$$k_{f(obs)} = \frac{K_I(k_1 + k_2a_{H^+})}{a_{H^+}} = k_2K_I + k_1K_I\frac{1}{a_{H^+}} \qquad \text{(Eq. 17)}$$

Consequently, k_1K_I and k_2K_I can be obtained from the slope and the ordinate intercept of a straight line when the observed formation rate constants are plotted against $1/a_{H^+}$. By dividing each value by K_I, the parameters k_1 and k_2 were estimated to be 7.38 × 10/min and 7.32×10^4/min M, respectively (Fig. 7). The parameters obtained are summarized in Table II.

A theoretical equation for the formation rate was obtained by putting these parameters into an equation which was derived by dividing both

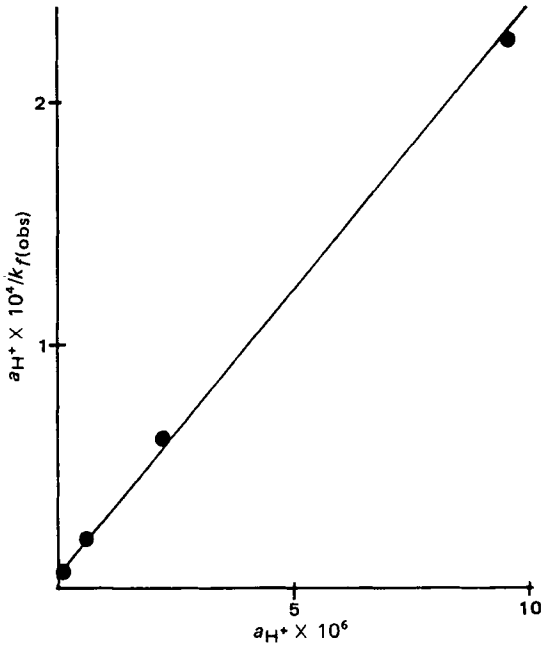

Figure 6—*Derivation of the constant* k_{-1}/k_1k_3 *and* K_I *by plotting rate data according to Eq. 12.*

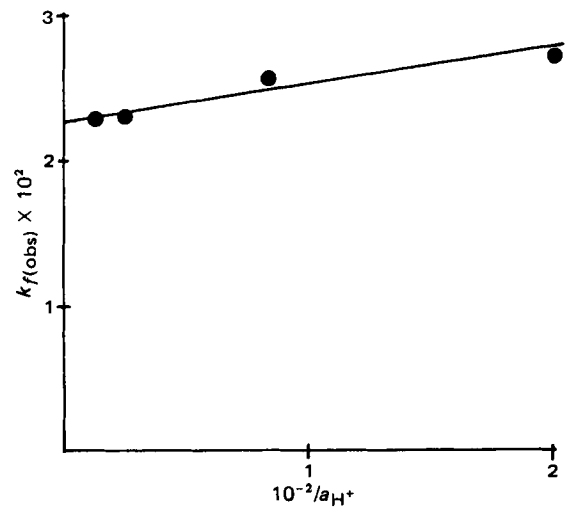

Figure 7—*Derivation of the rate constants* k_1 *and* k_2 *by plotting rate data according to Eq. 17.*

Table II—Kinetic Constants for the Equilibrium Reaction of Triazolam in Aqueous Buffer Solutions [a]

Parameter	Estimated Value	Parameter	Estimated Value
k_1, min^{-1}	7.38×10	k_3/k_{-1}, M^{-1}	1.88×10^3
k_2, $min^{-1}\ M^{-1}$	7.32×10^4	k_4/k_{-1}	5.42×10^{-5}
K_I, M	3.13×10^{-7}	$k_{-1}k_{-3}k_3$, min^{-1}	1.58×10^{-1}
k_1k_3/k_{-1}, $min^{-1}M^{-1}$	1.39×10^5	k_{-3}, $min^{-1}\ M^{-1}$	2.98×10^2
k_1k_4/k_{-1}, min^{-1}	4.0×10^{-3}	k_{-4}, min^{-1}	8.58×10^{-6}
k_4/k_3, M	2.88×10^{-8}	K_{II}, M	3.02×10^{-2}

[a] $\mu = 0.5$, at 37°.

denominator and numerator of Eq. 7 by k_{-1} (Eq. 18). The theoretical curve for the formation rate is shown as a solid line in Fig. 5. It satisfactorily fits the observed data over the pH range studied:

$$k_{f(obs)} = \frac{K_I(k_1 + k_2a_{H^+})\,(k_3a_{H^+}/k_{-1} + k_4/k_{-1})}{(K_I + a_{H^+})\,(1 + k_4/k_{-1} + k_3a_{H^+}/k_{-1})}$$
$$= 3.13 \times 10^{-7}\,(7.38 \times 10 + 7.32 \times 10^4 a_{H^+})\,\frac{(1.88 \times 10^3 a_{H^+} + 5.41 \times 10^{-5})}{(3.13 \times 10^{-7} + a_{H^+})\,(1 + 1.88 \times 10^3 a_{H^+})} \quad \text{(Eq. 18)}$$

Hydrolysis Mechanism—In the pH range studied, the term $(k_3a_{H^+} + k_4) \gg k_{-1}$, and Eq. 8 can be reduced to Eq. 19:

$$k_{r(obs)} = \frac{k_{-1}a_{H^+}\,(k_{-3}a_{H^+} + k_{-4})}{(K_{II} + a_{H^+})\,(k_3a_{H^+} + k_4)} \quad \text{(Eq. 19)}$$

In these pH solutions, the terms, $(k_3a_{H^+} + k_4)$ and $(k_{-3}a_{H^+} + k_{-4})$ are reduced to $k_3a_{H^+}$ and $k_{-3}a_{H^+}$, respectively, because the ratio k_4/k_3 or k_{-4}/k_{-3} is 2.88×10^{-8}, where the equilibrium constant of the second step in Scheme II can be represented by k_3/k_{-3} or k_4/k_{-4}. Therefore, Eq. 19 can be reduced to Eq. 20:

$$k_{r(obs)} = \frac{k_{-1}k_{-3}a_{H^+}}{k_3(K_{II} + a_{H^+})} \quad \text{(Eq. 20)}$$

Then Eq. 20 may be converted into the reciprocal form, Eq. 21:

$$\frac{1}{k_{r(obs)}} = \frac{k_3}{k_{-1}k_{-3}} + \frac{k_3K_{II}}{k_{-1}k_{-3}}\frac{1}{a_{H^+}} \quad \text{(Eq. 21)}$$

As shown in Fig. 8, plots of $1/k_{r(obs)}$ against $1/a_{H^+}$ gave a straight line with an intercept equal to $k_3/k_{-1}k_{-3} = 6.32$ min and a slope of $k_3K_{II}/k_{-1}k_{-3} = 0.191$ min M. Accordingly, K_{II} was estimated to be 3.02×10^{-2} ($pK_{II} = 1.52$). Furthermore, k_{-3} was calculated to be 2.98×10^2/min M from the $k_3/k_{-1}k_{-3}$ and k_3/k_{-1} values, which had already been known.

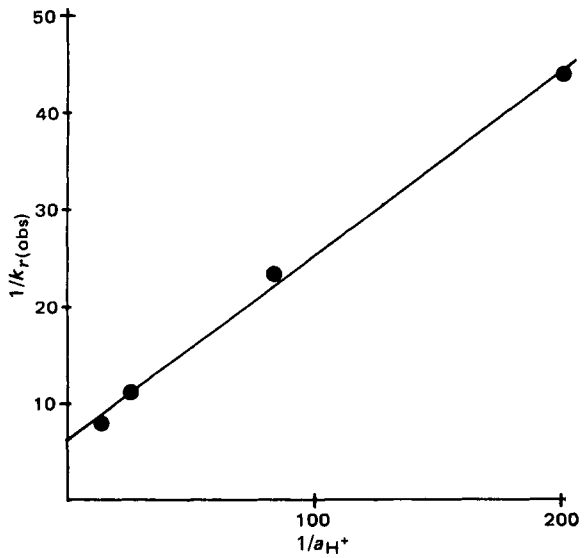

Figure 8—*Derivation of the constants* $k_3/k_{-1}k_{-3}$ *and* K_{II} *by plotting rate data according to Eq. 21.*

Also, $k_{-4} = 8.58 \times 10^{-6}$/min was obtained from the ratio of k_{-4}/k_{-3} and k_{-3}.

On the basic side of the formation rate maximum, no measurable hydrolysis rate constant has been obtained because the equilibrium exclusively favors the ring-closed form. Therefore, no information could be gained concerning the alkali hydrolysis.

A theoretical equation for the hydrolysis rate can be expressed as Eq. 22 by putting the parameters into the equation obtained after dividing both the denominator and the numerator of Eq. 8 by k_{-1}:

$$k_{r(obs)} = \frac{a_{H^+}(k_{-3}a_{H^+} + k_{-4})}{(K_{II} + a_{H^+})(1 + k_3a_{H^+}/k_{-1} + k_4/k_{-1})}$$
$$= \frac{a_{H^+}\,(2.98 \times 10^2/a_{H^+} + 8.58 \times 10^{-6})}{(3.02 \times 10^{-2} + a_{H^+})\,(1 + 1.88 \times 10^3\,a_{H^+})} \quad \text{(Eq. 22)}$$

The theoretical curve of Eq. 22 is shown in Fig. 5 as a solid line. The curve satisfactorily fits the observed reverse-reaction rate constants.

Equilibrium Constant—From the definition of the equilibrium, the Constant K is expressed by Eq. 23:

$$K = \frac{k_{f(obs)}}{k_{r(obs)}}$$
$$= \frac{K_I(K_{II} + a_{H^+})\,(k_1 + k_2a_{H^+})\,(k_3a_{H^+} + k_4)}{k_{-1}a_{H^+}\,(K_I + a_{H^+})\,(k_{-3}a_{H^+} + k_{-4})}$$
$$= \frac{K_I(K_{II} + a_{H^+})\,(k_1 + k_2a_{H^+})\,(k_3a_{H^+}/k_{-1} + k_4/k_{-1})}{a_{H^+}(K_I + a_{H^+})\,(k_{-3}a_{H^+} + k_{-4})}$$
$$= 3.13 \times 10^{-7}\,(3.02 \times 10^{-2} + a_{H^+})\,(7.38 \times 10 + 7.32 \times 10^4 a_{H^+})\,\frac{(1.88 \times 10^3 a_{H^+} + 5.42 \times 10^{-5})}{a_{H^+}\,(3.13 \times 10^{-7} + a_{H^+})\,(2.98 \times 10^2\,a_{H^+} + 8.58 \times 10^{-6})} \quad \text{(Eq. 23)}$$

The theoretical F_I and F_{II} curves obtained from Eqs. 4, 5, and 23 are given in Fig. 3 as solid lines. The theoretical curves showed good agreement with the observed data, in which K and F_I were calculated to be 0.15 and 0.87 at pH 0, respectively.

Evaluation of the Reaction Rate—For an aromatic Schiff base, the maximum formation rate of *N*-*p*-chlorobenzylideneaniline was calculated to be 3.72×10^{-3}/min, if the equimolar reaction of *p*-chlorobenzaldehyde with aniline would occur in an aqueous solution of pH 4.0 at 25° (18). The maximum reaction rate from I to II was 10 times larger than that of the above intermolecular reaction. Generally, an intramolecular reaction would occur much more rapidly than an intermolecular one because of the more feasible approach between the active sites (20). However, this result indicates that the difference between the formation rates of *N*-*p*-chlorobenzylideneaniline and of Compound II would not be as large as expected if the rate measurements were performed under the same reaction conditions. To compare the formation rates of II for intra- and intermolecular reactions, the reactions of substituted triazolobenzophenone with aminoacetic acid needed to be investigated.

The rates of hydrolysis of several 1,4-benzodiazepines into the corresponding amines have been obtained in 0.1 *N* HCl solution at 37°. The values were 2.5×10^{-3}/min for diazepam (8), 4.25×10^{-1}/min for estazolam (10), 1.5×10^{-2}/min for fludiazepam (11), and 1.30×10^{-1}/min for flurazepam (11). The hydrolysis rate for triazolam in this study, as well as the pKa value, were similar to that for flurazepam. Moreover, the water catalyzed rate constant of hydrolysis for II ($k_{-4} = 8.58 \times 10^{-6}$/min) was similar to those for demoxepam (2) and oxazepam (3).

General Discussion—The pKa for the conjugate acid of Compounds I and II was estimated to be 6.50 and 1.52, respectively. No information has been reported about the pKa's for these compounds because the reaction in aqueous solution is too fast for measurement of the dissociation constant spectrometrically. However, the pKa for 2-aminoacetamido-5-chlorobenzophenone has been reported to be 6.3 (12), which is nearly the same as that for I. These constants indicate that the basicities of the ring-opened compounds are somewhat stronger than that of hydroxylamine, pKa 6.0. On the other hand, the pKa for the conjugate acid of 1,4-benzodiazepines has been widely studied. As already known, the 1,4-benzodiazepines which possess a 2′-halogen substituent in the 5-phenyl group exhibit a pKa value lower than that for corresponding nonsubstituent compounds (21, 22). Namely, the pKa's for fludiazepam, flunitrazepam, and lorazepam were reported to be 2.29, 1.71, and 1.3, respectively, which were significantly lower than those of the corresponding compounds without halogen in the 2′-position, diazepam (pKa = 3.3), nitrazepam (pKa = 3.2), and oxazepam (pKa = 1.7). The pKa

value for 8-chloro-6-phenyl-4H-*s*-triazolo[4,3-*a*][1,4] benzodiazepine (estazolam) was reported to be 2.84 from the UV absorption spectral change (23). Considering the structural difference mentioned, the estimated pKa value for triazolam, 1.52, is reasonable.

The bioavailability or the pharmacological effect of a drug would greatly depend on the formation rate in the cyclization reaction from the opened form to the closed form because only the cyclized 1,4-benzodiazepines possess pharmacological CNS activity (24), which are discussed in reports on diazepam (8) and desmethyldiazepam (12). The half-time of the forward reaction of I at pH 7.4, which was calculated to be 80.6 min (Fig. 5), indicates that much time is required to convert I into the closed form II, only if the *in vivo* reaction proceeds chemically.

REFERENCES

(1) H. V. Maulding, J. P. Nazareno, J. E. Pearson, and A. F. Michaelis, *J. Pharm. Sci.*, **64**, 278 (1975).

(2) W. W. Han, G. J. Yakatan, and D. D. Maness, *ibid.*, **65**, 1198 (1976).

(3) *Ibid.*, **66**, 573 (1977).

(4) W. Mayer, S. Erbe, and R. Voigt, *Pharmazie*, **27**, 32 (1972).

(5) W. W. Han, G. J. Yakatan, and D. D. Maness, *J. Pharm. Sci.*, **66**, 795 (1977).

(6) W. Mayer, S. Erbe, G. Wolf, and R. Voigt, *Pharmazie*, **29**, 700 (1974).

(7) W. H. Hong, C. Johnston, and D. Szulczewski, *J. Pharm. Sci.*, **66**, 1703 (1977).

(8) M. Nakano, N. Inotsume, N. Kohri, and T. Arita, *Int. J. Pharm.*, **3**, 195 (1979).

(9) N. Inotsume and M. Nakano, *J. Pharm. Sci.*, **69**, 1331 (1980).

(10) N. Inotsume and M. Nakano, *Chem. Pharm. Bull.*, **28**, 2536 (1980).

(11) N. Inotsume and M. Nakano, *Int. J. Pharm.*, **6**, 147 (1980).

(12) H. Bundgaard, *Arch. Pharm. Chem. Sci. Ed.*, **8**, 15 (1980).

(13) W. P. Jencks, "Catalysis in Chemistry and Enzymology," McGraw-Hill, New York, N.Y., 1969, pp. 163–242, 463–554.

(14) W. P. Jencks, *Prog. Phys. Org. Chem.*, **2**, 63 (1964).

(15) R. B. Martin, *J. Phys. Chem.*, **68**, 1369 (1964).

(16) W. P. Jencks, *J. Am. Chem. Soc.*, **81**, 475 (1959).

(17) E. H. Cordes and W. P. Jencks, *ibid.*, **84**, 4319 (1962).

(18) *Ibid.*, **84**, 832 (1962).

(19) *Ibid.*, **85**, 2843 (1963).

(20) J. Hine, "Physical Organic Chemistry," McGraw-Hill, New York, N.Y., 1962, pp. 141–151.

(21) J. Barrett, W. F. Smyth, and I. E. Davidson, *J. Pharm. Pharmacol.*, **25**, 387 (1973).

(22) R. T. Hagel and E. M. Debesis, *Anal. Chim. Acta*, **78**, 439 (1975).

(23) H. Koyama, M. Yamada, and T. Matsuzawa, *J. Takeda Res. Lab.*, **32**, 77 (1973).

(24) M. Fujimoto, Y. Tsukinoki, K. Hirose, K. Hirai, and T. Okabayashi, *Chem. Pharm. Bull.*, **28**, 1374 (1980).

Extended Hildebrand Solubility Approach: Testosterone and Testosterone Propionate in Binary Solvents

A. MARTIN *x, P. L. WU *, A. ADJEI §, M. MEHDIZADEH ‡, K. C. JAMES ‡, and CARL METZLER *¶

Received October 9, 1981, from the **Drug Dynamics Institute, College of Pharmacy, University of Texas, Austin, TX 78712* and the ‡*Welsh School of Pharmacy, University of Wales, Institute of Science and Technology, Cardiff, CF1 3NU, United Kingdom.* Accepted for publication January 28, 1982.

§Present address: Abbott Laboratories, North Chicago, IL. ¶On leave from The Upjohn Co., Kalamazoo, MI.

Abstract □ Solubilities of testosterone and testosterone propionate in binary solvents composed of the inert solvent, cyclohexane, combined with the active solvents, chloroform, octanol, ethyl oleate, and isopropyl myristate, were investigated with the extended Hildebrand solubility approach. Using multiple linear regression, it was possible to obtain fits of the experimental curves for testosterone and testosterone propionate in the various binary solvents and to express these in the form of regression equations. Certain parameters, mainly K and $\log \alpha_2$, were employed to define the regions of self-association, nonspecific solvation, specific solvation, and strong solvation or complexation.

Keyphrases □ Testosterone—extended Hildebrand solubility approach, solubility in binary solvents □ Solubility—extended Hildebrand solubility approach, testosterone and testosterone propionate in binary solvents □ Binary solvents—solubility of testosterone and testosterone propionate, extended Hildebrand solubility approach

Solute–solvent complexes of testosterone and testosterone propionate in binary solvents composed of cyclohexane with ethyl oleate, isopropyl myristate, and octanol have been reported previously (1). These solvents are pharmaceutically important; the first two are useful as solvents for steroid injectable preparations.

The calculated complexation constants (1) between the steroids and solvents were based on a previous method (2). The solute-mixed solvent systems are analyzed here with the extended Hildebrand solubility approach (3), an extension of the Hildebrand regular solution theory (4) which was introduced to allow the calculation of solubility of nonpolar and semipolar drugs in mixed solvents having a wide range of solubility parameters.

THEORETICAL

Solubility on the mole fraction scale, X_2, may be represented by the expression:

$$-\log X_2 = -\log X_2^i + \log \alpha_2 \qquad \text{(Eq. 1)}$$

where X_2^i is the ideal solubility of the crystalline solid, and α_2 is the solute activity coefficient in mole fraction terms. Scatchard (5) and Hildebrand and Scott (4) formulated the solubility equation for regular solutions in the form:

$$\log \frac{a_2^s}{X_2} = \log \alpha_2 = \frac{V_2 \phi_1^2}{2.303RT}(a_{11} + a_{22} - 2a_{12}) \qquad \text{(Eq. 2)}$$

where

$$\phi_1 = \frac{V_1(1 - X_2)}{V_1(1 - X_2) + V_2 X_2} \qquad \text{(Eq. 3)}$$

The activity of the crystalline solid (a_2^s), taken as a supercooled liquid, is equal to X_2^i as defined in Eq. 1. Variable V_2 is the molar volume of the

0022-3549/82/1200-1334$01.00/0